

## ARTICLES

## Effect of Hexafluorobenzene on the Photophysics of Pyrene

Mark Perry, Claudio Carra, Michelle N. Chrétien,<sup>\*,†</sup> and J. C. Scaiano\*

Department of Chemistry, University of Ottawa, 10 Marie Curie, Ottawa, Canada K1N 6N5

Received: January 12, 2007; In Final Form: March 31, 2007

Absorption and fluorescence spectroscopy studies reveal the formation of a weak complex between pyrene and C<sub>6</sub>F<sub>6</sub> even in very dilute systems. The complex affects the photophysics of pyrene and reveals a combination of static and dynamic-quenching phenomena in both polar and nonpolar solvents. The results are supported by computational studies that shed light on the structure of the complex and the interactions involved and suggest that ground and excited-state interactions are of comparable magnitude; the association is believed to be driven by quadrupolar interactions. Understanding these interactions in solution is important for applications that aim at controlling the regio- or stereoselectivity of organic reactions.

## Introduction

Arene–perfluoroarene interactions have been a topic of interest since Prosser and Patrick first reported the serendipitous formation of a crystalline material from an equimolar mixture of benzene and hexafluorobenzene.<sup>1</sup> The solid complex has a melting point of 24 °C, approximately 19 °C higher than either of the two components. Complex formation is believed to result partially from quadrupolar interactions and the strength of the binding interaction has been estimated to be ~4 kcal/mol, comparable in magnitude to a moderate hydrogen bond.<sup>2</sup> Replacing the six hydrogen atoms of benzene with electronegative fluorine atoms results in a dramatic change of the quadrupole moment ( $Q$ ) to a value of similar magnitude but opposite sign; C<sub>6</sub>H<sub>6</sub> and C<sub>6</sub>F<sub>6</sub> have quadrupole moments of  $-29.0 \times 10^{-40}$  and  $31.7 \times 10^{-40}$  Cm<sup>-2</sup>, respectively.<sup>3</sup>

The unique character of this interaction has been the subject of considerable interest in recent years, and it has been exploited in a number of applications due to its predictable nature. Arene–perfluoroarene interactions have been used in crystal engineering, notably by Marder and co-workers,<sup>4,5</sup> and the predictability of crystal packing has been exploited for the preparation of electroluminescent materials<sup>6</sup> and the stabilization of liquid crystal phases.<sup>7</sup> The use of quadrupolar interactions as a supramolecular synthon in the solid state has been applied to the [2 + 2] photocyclization of crystalline *trans*-pentafluorostilbene.<sup>8</sup> Phenyl–perfluorophenyl interactions cause a preorientation of the starting materials in a head-to-tail fashion resulting in near quantitative yields of the photodimerization product with excellent stereocontrol. This work was further extended to the use of quadrupolar interactions to control cross-linking in hydrogels.<sup>9</sup> Examples of quadrupolar interactions in solution, especially in terms of synthetic utility, are much more rare. An early example is the catalyzed macrocyclization of acetylenic cyclophanes where arene–perfluoroarene interactions

were used to prejudice the system toward the formation of the desired intermediate.<sup>10</sup> The use of quadrupolar interactions as facilitating elements in organic synthesis has recently been elaborated by Collins et al. in the context of macrocyclizations via ring-closing metathesis (RCM).<sup>11</sup> In this case, phenyl–perfluorophenyl interactions act to reduce degrees of rotation in various benzyl ester paracyclophanes leading to facile RCM with the aid of a first generation Grubbs catalyst. These results complement various examples of face-selective addition/cycloaddition reactions involving similar  $\pi$ – $\pi$  interactions that have proven powerful tools for conformational control in organic synthesis.

The question of how to describe these types of interactions has also attracted the attention of computational chemists, and these complexes have been examined both as 1:1 pairs as well as in the infinite lattices of the crystalline material. Despite the abundance of computational and structural data on the complexes, direct evidence for complex formation in moderately dilute solution is lacking. Previous attempts to characterize this interaction by UV–visible, NMR, and Raman spectroscopies either failed or were inconclusive.<sup>12</sup> The examples given above, especially the recent solution-phase chemistry, demonstrate the utility of these noncovalent interactions in influencing reactivity, as well as regio- and stereoselectivity, and highlight the need for a better understanding of these systems. We have applied a spectroscopic probe to learn more about arene–perfluoroarene interactions in dilute solution.

Pyrene photophysics is among the best understood in organic photochemistry and the subject of frequent studies.<sup>13</sup> Its rich photophysics includes the formation of excited-state complexes, referred to as excimers,<sup>14</sup> at concentrations exceeding 1 mM. The vibrational structure of pyrene fluorescence has been widely employed as a probe for environmental polarity,<sup>15</sup> even in very dilute solutions. In this study, we take advantage of this well-understood photophysics and of our own experience with pyrene

<sup>†</sup> Current address: Xerox Research Centre of Canada, 2660 Speakman Drive, Mississauga Ontario, L5K 2L1, Canada.

to probe the solution-phase interaction between pyrene and C<sub>6</sub>F<sub>6</sub> using steady-state and time-resolved fluorescence techniques.

### Experimental and Computational Methods

Pyrene (99%) was obtained from Aldrich and recrystallized in 95% ethanol before use. Hexafluorobenzene (99%) was also obtained from Aldrich and was distilled before use. Acetonitrile and cyclohexane were both spectroscopic grade solvents obtained from Fischer Scientific and used as received.

UV–vis absorption spectra were obtained on a Varian Cary-50 spectrometer, and steady-state fluorescence emission spectra were obtained on a PTI luminescence spectrometer. Time-resolved fluorescence data were recorded with a customized Luzchem laser flash photolysis system similar to that described elsewhere.<sup>16</sup> This customized system uses standard Luzchem software, but the detection system employed a CVI DK-240 monochromator and a Hamamatsu R928 red-sensitive photomultiplier instead of the standard components. Samples were excited with 308 nm pulses from a Lumonics EX-530 excimer laser (6 ns pulse width, ~30 mJ/pulse at the sample). Five laser shots were averaged for each decay trace, and fluorescence lifetimes longer than 50 ns have typical errors of 3% for the main emission component.

Fluorescence measurements were carried out with solutions of 8 μM pyrene in spectroscopic grade acetonitrile or cyclohexane in fused quartz cuvettes from Luzchem Research with a 10 mm or 7 mm optical path for steady-state or time-resolved measurements, respectively. These solutions were deaerated for 20 min by nitrogen bubbling. Hexafluorobenzene was deaerated similarly and was added as a neat liquid in 5–10 μL increments to pyrene samples using a 10 μL Hamilton syringe.

Lifetime measurements in pure C<sub>6</sub>F<sub>6</sub> required the use of a faster system allowing deconvolution of the instrument response function. For these measurements we employed an Easylife spectrometer from PTI, equipped with a 340 nm excitation diode and using a 375 nm long pass filter before the detector. A single-exponential kinetic analysis (19.2 ns) gave a good fit. The use of a double exponential function improved only marginally suggesting a 2.4% contribution from a subnanosecond component.

To study the interaction between hexafluorobenzene and pyrene, we performed *ab initio* calculations using the Gaussian 03 series of programs.<sup>17</sup> All the stationary points considered were located using the Møller–Plesset second-order perturbation theory (MP2)<sup>18</sup> with the 6-31G\* basis set. The SCF bonding energy was BSSE corrected with the Counterpoise method developed by Boys and Bernardi.<sup>19</sup> On the optimized geometries, the traceless quadrupole moment tensor component perpendicular to the aromatic rings,  $Q_{zz}$ , was calculated by HF/6-31G\*\*<sup>20</sup> for the singlet ground state ( $S_0$ ) and first triplet excited state ( $T_1$ ) both on a B3LYP/6-31G\*\*<sup>21</sup> optimized geometry and by CIS/6-31G\*\*<sup>22</sup> for the first singlet excited state ( $S_1$ ). The units are expressed in DÅ, also called Buckingham (B), and are equivalent to  $1.602 \times 10^{-39} \text{ cm}^2$ .<sup>23</sup>

### Results

The interaction between pyrene and C<sub>6</sub>F<sub>6</sub> was examined in both cyclohexane and in acetonitrile. Pyrene concentrations were selected so as to avoid excimer formation and to obtain absorbances at the fluorescence excitation wavelength of 0.2 or less.

**Absorption Spectroscopy.** The addition of C<sub>6</sub>F<sub>6</sub> to solutions of pyrene in cyclohexane or acetonitrile resulted in minimal

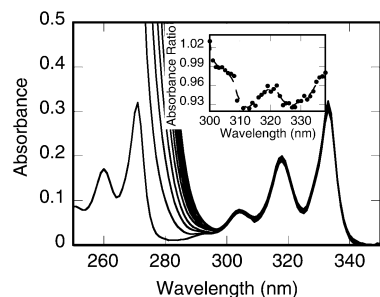


**Figure 1.** Absorption of 8 μM pyrene in acetonitrile with increasing concentrations of C<sub>6</sub>F<sub>6</sub> up to 0.14 M. Inset: absorbance ratio of pyrene with and without 0.14 M C<sub>6</sub>F<sub>6</sub>.

changes in the absorbance spectrum, other than the trivial changes below 290 nm reflecting the absorbance due to added C<sub>6</sub>F<sub>6</sub>. Figure 1 shows the corresponding spectra in acetonitrile, while the inset shows the ratio of absorbance in the presence and absence of 0.14 M C<sub>6</sub>F<sub>6</sub>. The ratio has been corrected for the 1.2% dilution due to the addition of C<sub>6</sub>F<sub>6</sub>. It is clear that there is some modification of the pyrene extinction coefficient in the presence of C<sub>6</sub>F<sub>6</sub>, particularly at wavelengths corresponding to the valleys between peaks (e.g., at 312 and 327 nm). These small but measurable changes suggest some degree of interaction between pyrene and C<sub>6</sub>F<sub>6</sub> in the ground state, an idea that is supported by subsequent observations reported herein.

**Computational Chemistry.** The association between aromatics and their fluorinated analogs has attracted the attention of theoreticians who have successfully modeled many systems, including the interaction between benzene and hexafluorobenzene and that of pyrene and hexafluorobenzene.<sup>5</sup> The calculations reported in this work were performed using MP2 because density functional theory was not well suited to describing weak, noncovalent interactions. Strong emphasis was given to quadrupole–quadrupole interactions as they play a major role in the formation of complexes between apolar molecules. Seven different initial geometrical arrangements of pyrene and C<sub>6</sub>F<sub>6</sub> were used (see Supporting Information). The noncovalent binding energy for the most stable complex was 7.2 kcal/mol, approximately 4 kcal/mol stronger than for the benzene–C<sub>6</sub>F<sub>6</sub> complex calculated with the same level of theory.<sup>24</sup> The most stable complex (Figure 2) has a short inter-ring distance of 3.03 Å, and the corresponding electrostatic potential was calculated by HF/6-31G\* (Figure 2, right). In uncomplexed pyrene, the negative electrostatic potential (red area) would be symmetrically distributed around the center of the molecule. Interestingly, the presence of C<sub>6</sub>F<sub>6</sub> polarizes the  $\pi$ -system of pyrene as demonstrated by the loss of symmetry in the charge distribution map shown in Figure 2 (right). This effect is a clear indication of a through space interaction.

Because we are interested in the spectroscopic consequences of this type of interaction, we also calculated the quadrupole moment tensor component perpendicular to the aromatic rings ( $Q_{zz}$ ) for the ground ( $S_0$ ) and first excited  $S_1$  and  $T_1$  states of pyrene to estimate the change in bonding energy upon absorption of a photon. According to the literature,<sup>25</sup> the best method to calculate  $Q_{zz}$  is by Hartree–Fock (HF) with basis sets that include the polarization functions, such as 6-31G\*\*, but not diffuse functions, which give a systematic overestimation of the value. In the ground state, the  $Q_{zz}$  for pyrene, optimized by B3LYP/6-31G\*, is  $-21.03 \text{ DÅ}$ ; this is significantly higher than the value for benzene ( $-8.5 \text{ DÅ}$ ). The change in the quadrupole

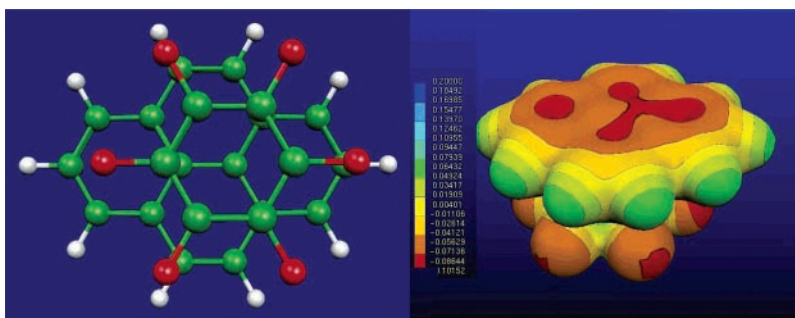


**Figure 2.** Optimized geometry of the most stable pyrene–C<sub>6</sub>F<sub>6</sub> complex (left) and the corresponding electrostatic potential calculated by HF/6-31G\* (right).

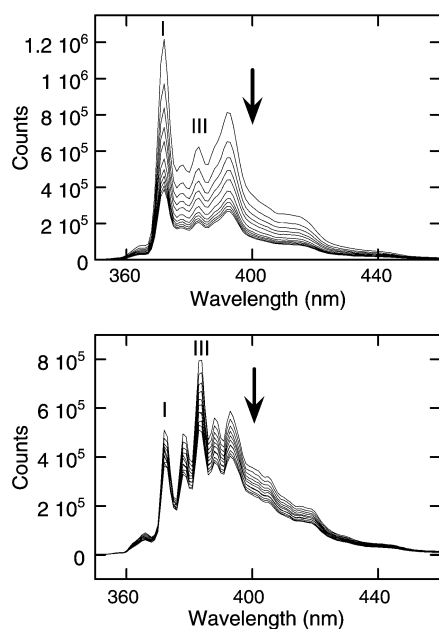


**Figure 3.** Steady-state fluorescence emission spectra of 8  $\mu$ M pyrene in acetonitrile (top) and cyclohexane (bottom) with concentrations of C<sub>6</sub>F<sub>6</sub> from 0 to 0.14 M.

moment on promotion to the excited state is minimal,  $-20.50$  DÅ for S<sub>1</sub> and  $-20.19$  DÅ for T<sub>1</sub>. This result suggests that the noncovalent bonding interaction is not extensively affected by electronic promotion to either the first singlet or triplet excited states.

**Fluorescence Spectroscopy.** In contrast to the minimal changes observed in the absorption spectra, C<sub>6</sub>F<sub>6</sub> has a significant effect on the fluorescence of pyrene, as revealed by both steady-state and time-resolved measurements. The pyrene concentrations selected were always low enough that excimer formation was not significant, thus leading to considerable simplification of the photophysics. Figure 3 shows the emission spectra of pyrene following 308 nm excitation recorded in the presence of various concentrations of C<sub>6</sub>F<sub>6</sub> in cyclohexane and in acetonitrile. The data points were acquired at 1 nm intervals. We note that the emission of pyrene is not completely suppressed even in pure C<sub>6</sub>F<sub>6</sub>. This spectrum has been included in the Supporting Information, and the integrated emission intensity is  $\sim 11\%$  of that in acetonitrile, corresponding to an emission quantum yield of 0.07 using the value in acetonitrile (0.62)<sup>26</sup> as a reference and applying the usual refractive index corrections.

The data at different C<sub>6</sub>F<sub>6</sub> concentrations were analyzed by applying a Stern–Volmer relationship to both the steady-state and time-resolved data as shown in Figure 4. In the case of a

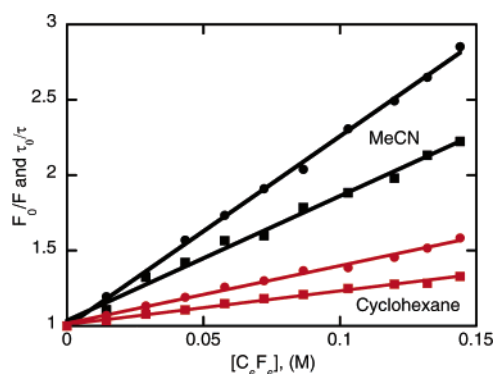


**Figure 4.** Steady-state (●) and time-resolved (■) Stern–Volmer analysis of pyrene (8  $\mu$ M) fluorescence quenching by C<sub>6</sub>F<sub>6</sub> in acetonitrile (black) and in cyclohexane (red).

purely dynamic-quenching interaction, eqs 1–3 are expected to hold

$$\frac{\Phi_0}{\Phi} = \frac{F_0}{F} = 1 + k_q\tau_0[Q] \quad (1)$$

$$\frac{\tau_0}{\tau} = 1 + k_q\tau_0[Q] \quad (2)$$

$$\frac{\Phi_0}{\Phi} = \frac{\tau_0}{\tau} \quad (3)$$

where  $\Phi$  and  $\tau$  are the quantum yield and lifetime of fluorescence and the subscript “0” indicates data in the absence of quencher;  $F_0$  and  $F$  are the experimental emission intensities,  $k_q$  is the rate constant for quenching, and  $[Q]$  the quencher concentration.

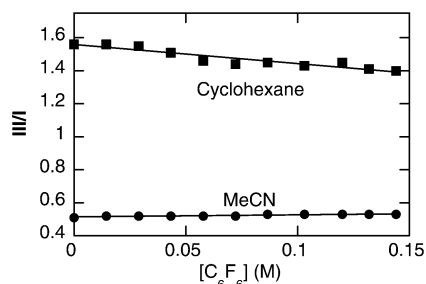
Stern–Volmer plots based on fluorescence intensities (eq 1) and on lifetimes (eq 2) are shown in Figure 4. It is clear that the equality of eq 3 does not hold. Simple systems involving a combination of dynamic and static quenching lead to curved plots (based on intensity) and frequently obey eq 4, where  $K_S$  is the association constant for interaction between fluorophore and quencher. By “simple” we refer to systems where a nonemissive complex is formed between fluorophore and quencher and where dissociation of the complex does not occur during the lifetime of its excited state.

$$\frac{\Phi_0}{\Phi} = 1 + (k_q\tau_0 + K_S)[Q] + K_S k_q\tau_0[Q]^2 \quad (4)$$

The plots from Figure 4 are reasonably linear, and the slopes are given in Table 1. The fact that eq 3 does not apply clearly indicates that the interaction is not simple dynamic quenching

**TABLE 1: Slopes Corresponding to Stern–Volmer Analysis Illustrated in Figure 4<sup>a</sup>**

	acetonitrile/M <sup>-1</sup>	cyclohexane/M <sup>-1</sup>
$\phi_0/\phi$	12.6 ± 0.4	3.8 ± 0.2
$\tau_0/\tau$	8.3 ± 0.5	2.2 ± 0.1

<sup>a</sup> Errors approximated as two standard deviations.**Figure 5.** Ratio of III/I vibronic bands from pyrene fluorescence in the presence of C<sub>6</sub>F<sub>6</sub> in acetonitrile and in cyclohexane.

and provides support for ground-state complexation between pyrene and C<sub>6</sub>F<sub>6</sub>.

The emission spectrum of pyrene has five distinct vibronic bands, and the ratio of the bands normally labeled I and III (see Figure 3) are frequently used as an indicator of polarity.<sup>15,27</sup> The change in this ratio with increasing concentrations of C<sub>6</sub>F<sub>6</sub> is illustrated in Figure 5; the variation, while small, is larger than anticipated given the low concentrations employed. When the values are extrapolated to pure C<sub>6</sub>F<sub>6</sub> (8.66 M), the two plots do not coincide (as they should). If one were to extrapolate the values to pure C<sub>6</sub>F<sub>6</sub>, they would be 1.59 when starting from acetonitrile and −8.4 when the initial solvent is cyclohexane. The experimental value in C<sub>6</sub>F<sub>6</sub> is 0.64. The extrapolated values are not meaningful, except to indicate the high sensitivity of pyrene's III/I band ratio in the presence of dilute C<sub>6</sub>F<sub>6</sub> where the degree of complexation is most affected by changes in C<sub>6</sub>F<sub>6</sub> concentration.

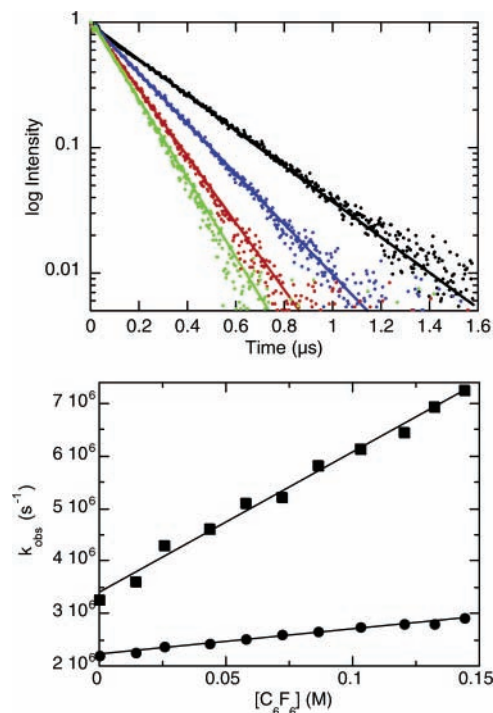
While linear extrapolation described above is of course a very rough approximation, it is consistent with the suggestion that there are specific interactions causing changes well in excess of those anticipated for typical solvent effects. Unfortunately, a full solvent survey is not practical for a variety of reasons including the limited miscibility of C<sub>6</sub>F<sub>6</sub> in many organic solvents.

**Time-Resolved Fluorescence Spectroscopy.** The same samples used for steady-state fluorescence spectroscopy were also employed to measure fluorescence lifetimes following 308 nm laser excitation. The concentrations of pyrene used were selected to avoid excimer formation, thus simplifying analysis of the data. In all cases, the fluorescence data were reasonably fitted with a monoexponential expression, as illustrated in Figure 6 (top) for representative C<sub>6</sub>F<sub>6</sub> concentrations. The slope of the graph of reciprocal fluorescence lifetime against the concentration of C<sub>6</sub>F<sub>6</sub> (Figure 6, bottom) gives the rate constant for quenching of the pyrene singlet state by C<sub>6</sub>F<sub>6</sub>. The measured values are  $2.7 \times 10^7 \text{ M}^{-1} \text{ s}^{-1}$  and  $4.8 \times 10^6 \text{ M}^{-1} \text{ s}^{-1}$  for acetonitrile and cyclohexane, respectively. Because the lifetime of the singlet state of pyrene in each solvent is known, the same information can be derived from the Stern–Volmer analysis shown in Figure 4 (see eq 2).

The lifetime in pure C<sub>6</sub>F<sub>6</sub> was 19.2 ns (see Experimental and Computational Methods for details).

## Discussion

The photochemistry and photophysics of pyrene are very well characterized making it an excellent probe for the spectroscopic

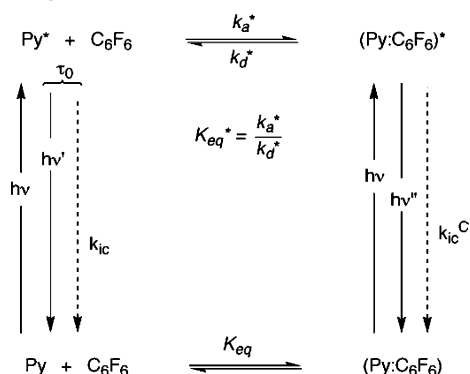
**Figure 6.** Time-resolved fluorescence data in acetonitrile and in cyclohexane. Top: semilogarithmic plot of signal intensity versus time for 0, 43, 103, and 144 mM C<sub>6</sub>F<sub>6</sub> in acetonitrile. Bottom: reciprocal lifetimes as a function of C<sub>6</sub>F<sub>6</sub> concentration illustrating the concentration-dependent quenching of pyrene fluorescence in cyclohexane (●) and acetonitrile (■).

examination of arene–perfluoroarene interactions in dilute solution. We have examined the changes in the absorption and emission behavior of pyrene in the presence of C<sub>6</sub>F<sub>6</sub>. The absorption spectrum of pyrene was modified in a small but consistent way upon the addition of C<sub>6</sub>F<sub>6</sub> (Figure 1) supporting the probable involvement of a ground-state pyrene–C<sub>6</sub>F<sub>6</sub> complex. This idea is supported by our computational study that indicated that complex formation is energetically favorable, as well as by literature data on the pyrene–C<sub>6</sub>F<sub>6</sub> crystal.<sup>5</sup>

Pyrene fluorescence is quenched by C<sub>6</sub>F<sub>6</sub> in both acetonitrile and cyclohexane (Figure 3). The bimolecular rate constants for pyrene fluorescence quenching,  $k_q$ , have been measured as  $2.7 \times 10^7 \text{ M}^{-1} \text{ s}^{-1}$  in acetonitrile and  $4.8 \times 10^6 \text{ M}^{-1} \text{ s}^{-1}$  in cyclohexane (Figure 6). Stern–Volmer analysis of the fluorescence-quenching data show (Figure 4) that plots of intensity ( $F_0/F$ ) and lifetime ( $\tau_0/\tau$ ) in cyclohexane and acetonitrile are reasonably linear, yet observably different (compare with eq 3). A combination of static and dynamic quenching is normally expected to result in curvature of the Stern–Volmer plot<sup>28</sup> (eq 4); however, small slopes, such as those reported here, tend to mask significant curvature. In principle, one could use hexafluorobenzene concentrations much higher than the 0.144 M employed in this work; however, we note that this would complicate the system by introducing significant solvent effects.

Equation 4 is a relevant contribution to the explanation of our results, however, this equation assumes the presence of irreversible complexes (static) whereas we assume an equilibrium between pyrene and C<sub>6</sub>F<sub>6</sub>. Ultimately, if the quenching interaction were exclusively static in nature and the ground-state complex nonemissive, we would expect the lifetime of the singlet excited state to be insensitive to quencher (C<sub>6</sub>F<sub>6</sub>) concentrations. This is clearly not the case, and the Stern–Volmer analysis based on emission lifetimes ( $\tau_0/\tau$ ) gives a positive linear slope (Figure 4), indicating that at least some

**SCHEME 1: Proposed Mechanism for the Pyrene/Hexafluorobenzene Preassociation and Quenching Behavior Exhibited in the Ground State and First Excited Singlet State<sup>a</sup>**



<sup>a</sup> The abbreviation Py is used for pyrene and the star (\*) indicates the lowest excited singlet state.

dynamic quenching is involved, requiring more than the formation of a nonemissive ground-state complex. In fact, even in pure  $C_6F_6$  pyrene still fluoresces with  $\sim 11\%$  efficiency, as compared to acetonitrile, and a fluorescence lifetime of 19.2 ns, compared to  $\sim 450$  and  $\sim 310$  ns in cyclohexane and acetonitrile, respectively.

As mentioned above, Stern–Volmer analysis of the fluorescence lifetime ( $\tau_0/\tau$ ) and the fluorescence intensity ( $F_0/F$ ) data show a linear relationship in both acetonitrile and cyclohexane. The magnitude of the Stern–Volmer constant (i.e., the slope) from the time-resolved data is different from the Stern–Volmer constant derived from the steady-state data (Table 1). Typical dynamic-quenching systems have Stern–Volmer constants from steady-state ( $F_0/F$ ) and time-resolved ( $\tau_0/\tau$ ) data that are virtually identical (eq 3), while purely static-quenching systems have a slope of  $\sim$ zero for  $\tau_0/\tau$  versus quencher concentration. The Stern–Volmer constants from the steady-state and time-resolved fluorescence quenching are significantly different in both acetonitrile and cyclohexane, indicative of a combination of preassociation and dynamic interaction between pyrene and  $C_6F_6$ . A schematic diagram of the proposed mechanism for quenching of pyrene fluorescence by  $C_6F_6$  is shown in Scheme 1.

The mechanism of Scheme 1 is deceptively simple. The observed emission in pure  $C_6F_6$  could result from either an emissive complex between pyrene and  $C_6F_6$  or from free pyrene in equilibrium with this complex; our data provide no compelling evidence for either possibility, or a combination of both. In either case, comparison of the lifetimes (19.2 versus 310 ns in acetonitrile) suggests that at least 94% of the pyrene will be present as its  $C_6F_6$  complex in pure (8.6 M)  $C_6F_6$ . The discussion that follows focuses on acetonitrile as a solvent, because the fluorescence III/I ratio is largely invariant in acetonitrile/ $C_6F_6$  solvent mixtures. Literature studies<sup>26</sup> indicate that radiative lifetime changes parallel changes in the III/I ratio; thus acetonitrile, with a III/I ratio comparable to  $C_6F_6$  (0.51 in acetonitrile versus 0.64 in  $C_6F_6$ ), is a better choice in terms of the approximations that this discussion requires. It is conceptually useful to base this analysis on one specific set of conditions, and we have chosen 0.1 M  $C_6F_6$  in acetonitrile. Examination of Figure 4 yields a  $\tau_0/\tau$  value of 1.87 for this concentration, corresponding to a lifetime of 166 ns (compare with 310 ns in the absence of quencher). If we assume complete excited-state equilibration (vide infra), then eq 5 allows the estimation of

“ $a$ ”, the fraction of pyrene complexed to  $C_6F_6$  in the excited-state equilibrium.

$$\frac{1}{\tau} = \frac{1}{166 \text{ ns}} = \frac{a}{310 \text{ ns}} + \frac{1-a}{19.2 \text{ ns}} \quad (5)$$

where the value of 19.2 ns is assumed to be the lifetime for the  $(\text{Py}/C_6F_6)^*$  complex and corresponds to the value measured in pure  $C_6F_6$ , clearly an approximation. On the basis of eq 1, we estimate  $a = 0.94$ , indicating that only ca. 6% of the excited pyrene is complexed to  $C_6F_6$  at a concentration of 0.1 M  $C_6F_6$ . From this the value of  $K_{eq}^*$  (see Scheme 1) is estimated as  $0.6 \text{ M}^{-1}$ . The estimated value would be higher if the lifetime of the  $(\text{Py}/C_6F_6)^*$  complex were longer than 19.2 ns. The low value of  $K_{eq}^*$  is consistent with the failure of earlier attempts to detect complexation in dilute solutions.

When we examine the Stern–Volmer plot based on emission intensities under the same experimental conditions as above (see Figure 4), we obtain  $F_0/F = 2.23$  for 0.1 M  $C_6F_6$  in acetonitrile, compared with 1.87 from the lifetime plot (vide supra). In a conventional Stern–Volmer plot, a  $F_0/F = 2.23$  corresponds to 55% quenching or 45% of the excited states escaping quenching. In fact, if we assume that quenching events still lead to about 11% of the fluorescence yield relative to the unquenched species (as suggested by the emission in pure  $C_6F_6$ ), then the fraction that escapes quenching is only 38%. While Scheme 1 does not require the equality of eq 3 to hold, the differences in this case cannot be fully accommodated within an equilibrium situation in the excited-state manifold ( $K_{eq}^*$ ) and requires that some static-quenching be involved. That is, some of the  $(\text{Py}/C_6F_6)^*$  complexes will decay before the excited-state equilibrium is fully established. Roughly, this means that  $k_d^*$  should be comparable or smaller than the reciprocal lifetime of the complex as measured by time-resolved fluorescence spectroscopy, that is,  $k_d^* \leq (19.2 \text{ ns})^{-1}$ .

It is easy to estimate if this is a reasonable condition by estimating a preexponential factor for the dissociation of the complex, and calculating the minimum activation energy required for dissociation. On a first approximation, we assume the preexponential factor  $A_d \sim 10^{13} \text{ s}^{-1}$ , leading to eq 6

$$k_d^* \leq (19.2 \times 10^{-9} \text{ s})^{-1} = 10^{13} \text{ s}^{-1} \exp(-Ea/RT) \quad (6)$$

corresponding to  $Ea \geq 7.3 \text{ kcal/mol}$  for  $(\text{Py}/C_6F_6)^*$  complex dissociation. Remarkably, this value compares well with the binding energy of 7.2 kcal/mol estimated by computational chemistry. These studies also suggest that the structure of the complex and its binding should be comparable in the ground and excited states; that is,  $K_{eq}^*$  and  $K_{eq}$  are probably not very different, implying that the contribution from pre-equilibration decay (eq 6) cannot be too large. This is consistent with the absence of a detectable fast component in the experimental fluorescence decays (see Figure 6, top) and probably reflects both the fact that this component is small and that its emission intensity is only 11% of that for uncomplexed pyrene.

Finally, the results are consistent with modest binding, as suggested by the computational studies, and are in line with the absence of significant shifts in the absorption or emission wavelengths observed. Not only are enthalpic terms similar for ground and excited states, but most likely there are only minor entropic changes related to excitation, because these usually relate to conformational changes<sup>29</sup> and are unimportant for rigid molecules such as pyrene and  $C_6F_6$ .

In conclusion, from the preceding discussion, while necessarily speculative, some points emerge clearly. For the first time,

data have been obtained that confirm the existence of a complex between aromatic molecules, pyrene in our case, and C<sub>6</sub>F<sub>6</sub> in dilute solution. However, the binding constant is small, estimated at ca. 0.6 M<sup>-1</sup> in this case. In the pyrene system, the equilibrium constants in the ground and excited state are similar, although their difference contributes to quenching in the form of a static component that precedes excited-state equilibration. Kinetic analysis is consistent with a binding energy around 7.2 kcal/mol, as estimated using computational methods. We note that early pre-equilibration phenomena is not expected to influence our discussion (vide supra) of the time-resolved data, because these data were obtained largely (see Figure 6, top) on time-scales involving several hundred nanoseconds where such early phenomena are complete.

Each of the examples given in the introduction, especially the recent use of arene–prefluoroarene interactions in solution-phase organic synthesis, highlight the need for a better understanding of quadrupolar interactions. The data presented here, while exploratory in nature, add to our understanding of these noncovalent interactions in dilute solution. Ultimately, we hope to expand our understanding of quadrupolar interactions to extend their utility, beyond crystal engineering, to their general use in controlling chemical reactivity.

**Acknowledgment.** We acknowledge the generous financial support of the Natural Sciences and Engineering Research Council (NSERC), the Canadian Foundation for Innovation, and the Government of Ontario. M.N.C. thanks NSERC for a postdoctoral fellowship.

**Supporting Information Available:** Additional computational details and pyrene fluorescence spectrum in pure C<sub>6</sub>F<sub>6</sub>. This material is available free of charge via the Internet at <http://pubs.acs.org>.

## References and Notes

- (1) Patrick, C. R.; Prosser, G. S. *Nature* **1960**, *187*, 1021.
- (2) (a) Overell, J. S. W.; Pawley, G. S. *Acta Crystallogr., Sect. B* **1982**, *38*, 1966. (b) Williams, J. H.; Cockcroft, J. K.; Fitch, A. N. *Angew. Chem., Int. Ed.* **1992**, *31*, 1655.
- (3) Battaglia, M. R.; Buckingham, A. D.; Williams, J. H. *Chem. Phys. Lett.* **1981**, *78*, 421.
- (4) (a) Batsanov, A. S.; Collings, J. C.; Howard, J. A. K.; Marder, T. B. *Acta Crystallogr., Sect. E* **2001**, *57*, 950. (b) Collings, J. C.; Roscoe, K. P.; Thomas, R. L.; Batsanov, A. S.; Stimson, L. M.; Howard, J. A. K.; Marder, T. B. *New J. Chem.* **2001**, *25*, 1410. (c) Collings, J. C.; Batsanov, A. S.; Howard, J. A. K.; Marder, T. B. *Cryst. Eng.* **2002**, *5*, 37.
- (5) Collings, J. C.; Roscoe, K. P.; Robins, E. G.; Batsanov, A. S.; Stimson, L. M.; Howard, J. A. K.; Clark, S. J.; Marder, T. B. *New J. Chem.* **2002**, *26*, 1740.
- (6) (a) Renak, M. L.; Bartholomew, G. P.; Wang, S.; Ricatto, P. J.; Lachicotte, R. J.; Bazan, G. C. *J. Am. Chem. Soc.* **1999**, *121*, 7787. (b) Strehmel, B.; Sarker, A. M.; Malpert, J. H.; Strehmel, V.; Seifert, H.; Neckers, D. C. *J. Am. Chem. Soc.* **1999**, *121*, 1226.
- (7) Weck, M.; Dunn, A. R.; Matsumoto, K.; Coates, G. W.; Lobkovsky, E. B.; Grubbs, R. H. *Angew. Chem., Int. Ed.* **1999**, *38*, 2741.
- (8) Coates, G. W.; Dunn, A. R.; Henling, L. M.; Ziller, J. W.; Lobkovsky, E. B.; Grubbs, R. H. *J. Am. Chem. Soc.* **1998**, *120*, 3641.
- (9) Kilbinger, A. F. M.; Grubbs, R. H. *Angew. Chem., Int. Ed.* **2002**, *41*, 1563.
- (10) Marsella, M. J.; Wang, Z.-Q.; Reid, R. J.; Yoon, K. *Org. Lett.* **2001**, *3*, 885.
- (11) (a) Collins, S. K.; El-azizi, Y. *Pure Appl. Chem.* **2006**, *78* (4), 783. (b) El-azizi, Y.; Schmitzer, A.; Collins, S. K. *Angew. Chem., Int. Ed.* **2006**, *45*, 968.
- (12) (a) Beaumont, T. G.; Davis, K. M. C. *J. Chem. Soc. B* **1967**, 1131. (b) Hwang, H. J.; Kim, K.; Kim, M. S. *Bull. Korean. Chem. Soc.* **1984**, *5* (6), 245.
- (13) Winnik, F. M. *Chem. Rev.* **1993**, *93*, 587.
- (14) Förster, T. Excimers and Exciplexes. In *The Exciplex*; Gordon, M., Ware, W. R., Eds.; Academic Press: New York, 1975; pp 1.
- (15) (a) Kalyanasundaram, K.; Thomas, J. K. *J. Am. Chem. Soc.* **1977**, *99*, 2039. (b) Dong, D. C.; Winnik, M. A. *Photochem. Photobiol.* **1982**, *35*, 17. (c) Dong, D. C.; Winnik, M. A. *Can. J. Chem.* **1984**, *62* (11), 2560.
- (16) Heyne, B.; Maurel, V.; Scaiano, J. C. *Org. Biomol. Chem.* **2006**, *4*, 802–807.
- (17) Frisch, M. J.; Trucks, G. W.; Schlegel, H. B.; Scuseria, G. E.; Robb, M. A.; Cheeseman, J. R.; Montgomery, J. A.; Vreven, T.; Kudin, K. N.; Burant, J. C.; Millam, J. M.; Iyengar, S. S.; Tomasi, J.; Barone, V.; Mennucci, B.; Cossi, M.; Scalmani, G.; Rega, N.; Petersson, G. A.; Nakatsuji, H.; Hada, M.; Ehara, M.; Toyota, K.; Fukuda, R.; Hasegawa, J.; Ishida, M.; Nakajima, T.; Honda, Y.; Kitao, O.; Nakai, H.; Klene, M.; Li, X.; Knox, J. E.; Hratchian, H. P.; Cross, J. B.; Bakken, V.; Adamo, C.; Jaramillo, J.; Gomperts, R.; Stratmann, R. E.; Yazyev, O.; Austin, A. J.; Cammi, R.; Pomelli, C.; Ochterski, J. W.; Ayala, P. Y.; Morokuma, K.; Voth, G. A.; Salvador, P.; Dannenberg, J. J.; Zakrzewski, V. G.; Dapprich, S.; Daniels, A. D.; Strain, M. C.; Farkas, O.; Malick, D. K.; Rabuck, A. D.; Raghavachari, K.; Foresman, J. B.; Ortiz, J. V.; Cui, Q.; Baboul, A. G.; Clifford, S.; Cioslowski, J.; Stefanov, B. B.; Liu, G.; Liashenko, A.; Piskorz, P.; Komaromi, I.; Martin, R. L.; Fox, D. J.; Keith, T.; Al-Laham, M. A.; Peng, C. Y.; Nanayakkara, A.; Challacombe, M.; Gill, P. M. W.; Johnson, B.; Chen, W.; Wong, M. W.; Gonzalez, C.; Pople, J. A. *Gaussian 03*, revision C.02; Gaussian, Inc.: Wallingford, CT, 2004.
- (18) Head-Gordon, M.; Pople, J. A.; Frisch, M. J. *Chem. Phys. Lett.* **1988**, *153*, 503.
- (19) Boys, S. F.; Bernardi, F. *Mol. Phys.* **1970**, *19*, 553.
- (20) Hehre, W. J.; Ditchfield, R.; Pople, J. A. *J. Chem. Phys.* **1972**, *56*, 2257.
- (21) Becke, A. D. *Phys. Rev. A* **1988**, *38*, 3098.
- (22) Foresman, J. B.; Head-Gordon, M.; Pople, J. A.; Frisch, M. J. *J. Phys. Chem.* **1992**, *96*, 135.
- (23) Glaser, R.; Lewis, M.; Wu, Z. *J. Phys. Chem. A* **2002**, *106*, 7950.
- (24) (a) Meyer, E. A.; Castellano, R. K.; Diederich, F. *Angew. Chem., Int. Ed.* **2003**, *42*, 1210. (b) Hunter, C. A.; Lawson, K. R.; Perkins, J.; Urch, C. J. *J. Chem. Soc., Perkin Trans. 2* **2001**, 651. (c) Hernández-Trujillo, M.; Costas, M.; Vela, A. *J. Chem. Soc., Faraday Trans.* **1993**, *89* (14), 2441.
- (25) (a) Heard, G. L.; Boyd, R. J. *Chem. Phys. Lett.* **1997**, *277*, (1–3), 252. (b) Hernandez-Trujillo, J.; Vela, A. *J. Phys. Chem.* **1996**, *100* (16), 6524.
- (26) Karpovich, D. S.; Blanchard, G. J. *J. Phys. Chem.* **1995**, *99* (12), 3951.
- (27) Nakajima, A. *Bull. Chem. Soc. Jpn.* **1971**, *44*, 3272.
- (28) Lakowicz, J. R. *Principles of Fluorescence Spectroscopy*; Springer Publishing: New York, 2006.
- (29) Gessner, F.; Scaiano, J. C. *J. Am. Chem. Soc.* **1985**, *107*, 7206.